Applied Catalysis B: Environmental 164 (2015) 443–452

Contents lists available at ScienceDirect

Applied Catalysis B: Environmental

journal homepage: www.elsevier.com/locate/apcatb

Cu and Co oxides supported on halloysite for the total oxidation of toluene

A.M. Carrillo, J.G. Carriazo*

Estado Sólido y Catálisis Ambiental (ESCA), Chemistry Department, Faculty of Science, National University of Colombia, Carrera 30 No. 45-03, Bogotá, Colombia

ARTICLE INFO

Article history:
Received 4 May 2014
Received in revised form 6 September 2014
Accepted 13 September 2014
Available online 22 September 2014

Keywords:
Toluene oxidation
Cobalt catalyst
Copper catalyst
Halloysite
Supported catalyst

ABSTRACT

This paper shows the chemical, structural and textural characterization of materials obtained from chemical modification of a clay mineral (halloysite) with species of Cu, Co and Cu—Co. The synthesized materials were characterized by elemental, structural and textural analyses using X-ray fluorescence (XRF), X-ray diffraction (XRD), temperature programmed reduction (H_2-TPR), N_2-adsorption and transmission electron microscopy (TEM). The catalytic performance was evaluated on the complete combustion of toluene, a model molecule of volatile organic compounds (VOCs). The characterization results showed the effective incorporation of chemical species of the metals used and the formation of copper oxides, cobalt oxides or mixed oxides as active phases of the catalysts. In addition, the XRD and TEM analyses indicated the structural and morphological conservation of the catalytic support (halloysite). The N_2-adsorption analysis showed that, in general, the type of porosity is maintained and predominantly determined by the support, although a reduction in a specific pore population was detected. The catalytic activity tests showed excellent performance of the materials as catalysts of the studied reaction, and revealed a cooperative effect due to the simultaneous incorporation of copper and cobalt species: the catalysts containing copper and cobalt were substantially more active than the catalysts containing only one metal in the oxide phase.

1. Introduction

The presence of volatile organic compounds (VOCs) in the atmosphere, mainly generated by poorly controlled industrial emissions, constitutes a risk to human health. These emissions induce the formation of ozone and photochemical smog by the action of solar light, which leads to severe environmental damage. VOCs, in addition to being toxic, carcinogenic, and teratogenic, are involved in the greenhouse effect [1,2].

There are several methods for VOC removal, among which catalytic oxidation offers some advantages. It occurs at moderate temperatures (165–440 °C), which allow lower operating costs; in addition, gas flows with low oxygen content are required, and the formation of NO_x in the combustion process is decreased [3–5]. Currently, the catalysts used to reduce VOC emissions can be divided into two categories: supported noble metals and bulk or supported metal oxides [6]. Catalysts of noble metals such as Pt and Pd are generally more active than transition metal oxide catalysts [4,7,8]. However, although the latter shows less catalytic activity at low temperatures than the noble metals, they are much cheaper and allow a greater catalyst loading, which leads to a larger active surface. Thus, metal oxide catalysts are only slightly less favorable than the noble metals for the oxidation of hydrocarbons [9]. In addition, metal oxide catalysts are characterized by high electronic mobility and metal ions with positive oxidation states.

Among the most studied metal oxides, cobalt catalysts have shown to be efficient in a wide range of reactions [10–12] due to the presence of mobile oxygen inside their spinel type structure (Co_3O_4) [13–17]. The high activity of this oxide in the removal of VOCs is due to its excellent reduction ability, its oxygen vacancies [18] and the high concentration of electrophilic oxide species (O_{ads}, O^- or O_2^-) [19] produced by the relatively low Co—O bond energy, which generates an easy interaction between the oxygen atoms in the lattice and the reactants [1]. However, its activity depends, among other factors, on the preparation conditions, the crystallization level, the cobalt oxidation state, and the surface area of the material [20].

It is believed that the total oxidation mechanism of hydrocarbons is a redox process in which the determining step is the

* Corresponding author at: Carrera 30 No. 45-03, Ciudad Universitaria, Edificio 451, oficina 109, Bogotá, Colombia. Tel.: +57 1 3165000x14403; fax: +57 1 3165220.
E-mail address: jcarriazog@unal.edu.co (J.G. Carriazo).

http://dx.doi.org/10.1016/j.apcatb.2014.09.027
0926-3373/

rate of oxygen removal from the metal oxide [21]. Therefore, the reducibility of the metal oxides seems to be one of the most critical parameters affecting the catalytic performance of VOC oxidation [21]. The reducibility of a metal oxide, and therefore its catalytic activity, can be improved by incorporating a second cation, i.e. by using a binary metal oxide catalyst [6]. It is established in the literature that the addition of CuO improves the catalytic activity of cobalt oxide in oxidation reactions [22,23]. These results suggest that the improvement in the catalytic conversion is due to the coexistence of Cu(II) and Co(III)/Co(II) ions in the system and to the synergic [24] and/or cooperative effects between cobalt and copper ions [22,23].

In turn, it is known that the deposition of a metal oxide in an adequate support leads to a material with better catalytic performance than a bulk catalyst, which can be explained by a greater dispersion of the active phase on the support. The recent use of nanotubular materials as catalytic supports is gaining increasing research interest. These nanotubes are an excellent support model to obtain active centers in form of nanoparticles inside the tubes [25]. However, in comparison with carbon nanotubes and boron nitride nanotubes, halloysite nanotubes (HNT) are natural, economical, and abundant. Halloysite can be considered a hydrated phase of kaolinite, with a general formula $Si_2Al_2O_5(OH)_4{\cdot}2H_2O$, and it can adopt different morphologies such as spheres, tubes, plates or slats. The elongated tubular morphology is usually the most stable, generating a nanometric cavity instead of a structure of stacked planes [26–28]. The HNT structure is composed of two aluminosilicate units: a sheet of tetrahedrons, type $(SiO_4)^{4-}$, that are located in the outer surface, exposing Si—O and Si—OH groups; and a sheet of octahedrons usually constituted by Al^{3+} and O^{2-} anions, with OH^- on the inner surface (Al—OH) [29,30]. These surface groups are potential sites for anchoring particles that can act as active phase in a heterogeneous catalyst [31–34]. However, research on halloysite nanotubes as a catalytic support remains scarce.

In this work, catalysts of Co and/or Cu oxides supported on halloysite nanotubes were designed for the total oxidation of toluene, which is a VOC widely used as industrial solvent. This study is intended to advance on designing of catalysts for the oxidation of VOCs with high conversions to CO_2. Catalysts with elevated thermal stability, resistance to sintering and low production costs are desired. In addition, this work contributes to the worldwide efforts to make rational use of natural resources and develop new technologies for environmental protection in moderate conditions of pressure and temperature.

2. Materials and methods

2.1. Catalyst synthesis

The halloysite type clay was obtained from Mondoñedo, a mine located near Bogotá, in the department of Cundinamarca (Colombia). This mineral was ground and sieved in 100-ASTM mesh (125–150 μm). A set of catalysts was synthesized by the wet impregnation method, using aqueous solutions of $Co(NO_3)_2{\cdot}6H_2O$ (Panreac 99%) and $Cu(NO_3)_2{\cdot}3H_2O$ (Panreac 99%). Two series of materials were obtained by varying the Cu/Co molar ratio (0/4, 1/1, 2/1, 1/2, and 4/0), and maintaining a 4 mmol of metal/g of halloysite nominal loading, equivalent to a total metal loading of approximately 20 wt%. Afterwards, catalysts with Cu/Co molar ratios of 1/1 and 1/2 were obtained by varying the total metal loading between 10 and 40 wt%. All prepared catalysts were dried at 60 °C for 24 h and calcined at 400 °C for 2 h in static air atmosphere. The nomenclature used for the synthesized catalysts is described in Table 1, where numbers before each chemical symbol indicate the Cu/Co molar ratio. Thus, the 0Cu4Co/H catalyst refers to the material prepared with only cobalt supported on halloysite, and the 1Cu2Co/H solid refers to the material prepared with a Cu/Co molar ratio equal to 1/2.

2.2. Characterization

Chemical analysis was performed by X-ray fluorescence (XRF) using a Magix Pro PW-2440 spectrometer equipped with a rhodium tube and with a maximum power of 4 kW. The X-ray diffraction profiles were collected at room temperature using a Panalytical X'Pert PRO MPD (Cu Kα radiation, λ = 1.54056 Å) instrument with 2θ geometry, from 5° 2θ to 80° 2θ, step size of 0.01° and step time of 10 s.

Temperature programmed reduction (H_2-TPR) experiments were carried out using a Chembet 300 (Quantachrome) equipment, with quartz reactor and thermal conductivity detector (TCD). Hydrogen (99.995%, Agafano, Colombia) as reducing agent, and argon (99.998%, Agafano, Colombia) as carrier gas were used. Samples were previously degassed at 150 °C for 1 h under argon flow. The analyses were performed with 10 °C/min heating rate, a mixture of 10% v/v (3.1 mmol H_2/cm^3) H_2/Ar, and 0.27 mL (STP)/s flow.

Transmission electron micrographs (TEM) were obtained using an FEI electronic microscope, TECNAI 20 Twin–200 kV model. The materials were suspended in ethanol by sonication; the suspended particles were deposited on a copper grid and dried at room temperature.

The nitrogen adsorption isotherms were performed at 77 K using a Micromeritics ASAP 2020 equipment, in the interval of relative pressures (P/P_0) from 1×10^{-5} to 0.99. Prior to each analysis, the samples were degassed at 200 °C for 24 h.

2.3. Catalytic evaluation

The catalytic performance was evaluated using a fixed bed U-shaped glass reactor that operates in continuous flow at atmospheric pressure. The catalytic conversion was investigated as a temperature function, for which a total flow of 200 mL/min, 0.200 g of catalyst (sieved at 125–150 μm), a toluene concentration of 600 ppm, supplied by a permeable unit, and synthetic air as an oxidizing agent were used. The catalysts were pretreated in air flow at 400 °C for 2 h. The catalytic conversion curves were obtained by cooling at 1.5 °C/min from 400 to 100 °C. The disappearance of the reactant and the formation of products were analyzed in line with a gas chromatograph (GC-17A–Shimadzu) equipped with a BPX-Volatiles column and a FID detector. The yield to CO_2 was measured using a Bacharach CO_2 analyzer, 3150 model, equipped with an IR detector.

3. Results and discussion

3.1. Effect of the Cu/Co molar ratio

3.1.1. Chemical analysis

The elemental chemical analysis (Table 1) confirms the effective incorporation of copper and cobalt metals in the supported catalysts, according to the expected results. A weight ratio of SiO_2/Al_2O_3 greater than 1.2 for the clay mineral indicates a smaller amount of Al_2O_3 with respect to the corresponding amount of SiO_2, most likely due to the presence of silica impurities. Likewise, small amounts of calcium, sodium, iron, and titanium were found, among other elements, which frequently come with this clay mineral, either as components of its structure or as contaminants.

3.1.2. X-ray diffraction

The X-ray diffraction profiles of the synthesized catalysts (Fig. 1) show characteristic signals of copper (CuO) and cobalt (Co_3O_4)

Table 1
Elemental chemical analysis of copper and cobalt into the supported catalysts, and their comparison with the support (halloysite).

Solid	SiO_2/Al_2O_3	Other metals[b]	% Co	% Cu	% Cu + % Co	$(Cu + Co)_{theoretical}$ [a]	Relative error (%)
Halloysite	1.310	2.081	–	–	–	–	
4Cu0Co/H	1.160	1.293	0.003	19.773	19.776	20.259	2.38
2Cu1Co/H	1.196	1.485	6.221	14.440	20.661	21.755	5.03
1Cu1Co/H	1.226	1.505	9.039	11.006	20.045	21.768	7.91
1Cu2Co/H	1.241	1.481	12.368	7.375	19.743	21.423	7.84
0Cu4Co/H	1.232	1.529	19.312	0.047	19.359	19.072	1.50

[a] Calculated values (%) taking into account the quantities used on the synthesis of each solid.
[b] The sum of Na, Ca, K, Fe, Mg and Ti contents.

oxides [35]. The intensities of these signals increase as the loading of each metal is increased. This result preliminarily indicates the successful formation of such metallic oxides at 400 °C. In addition, the characteristic signals of the support were observed, which verifies the structural stability of the clay mineral during the synthesis. For those materials that contain cobalt oxide, the 19° 2θ signal indicates the presence of Co_3O_4 and/or oxide phases such as $CoAl_2O_4$ or Co_2AlO_4 [36].

3.1.3. Temperature programmed reduction

The catalytic oxidation of VOCs is a redox process involving metal species varying their oxidation states. For that, the performance of catalysts in such reactions can be associated with the ability of these metal species to be reduced. Fig. 2 shows the H_2-TPR profiles of (20 wt%) Cu—Co/halloysite catalysts with different Cu/Co molar ratio. All the catalysts have reduction temperatures lower than 500 °C, with the exception of the material 0Cu4Co/H. For this catalyst the first zone between 200 and 500 °C is attributed to redox processes of cobalt oxide to form metal cobalt [10].

$$Co_3O_4 + H_2 \rightarrow 3CoO + H_2O$$

$$3CoO + 3H_2 \rightarrow 3Co^0 + 3H_2O$$

In this way, the peaks observed at 350 °C and 430 °C for the material 0Cu4Co/H were associated with the reductions of Co_3O_4 to CoO and then to Co^0 [37]. Additionally, because of TPR is a complex process, a second phenomenon can be involved in the second peak (430 °C) because Co^{2+}/Co^{3+} species of less accessibility (both inner sites and oxide particles with higher size) can also be reduced about this temperature [38], allowing the formation of a broader signal. Another broad signal at high temperature (550–700 °C) may correspond to the total reduction of phases $CoAl_2O_4$ or Co_2AlO_4 [39] formed as consequence of a strong metal-support interaction.

On the other hand, the TPR profile of 4Cu0Co/H shows a signal at 328 °C, which is assigned to the reduction of CuO species to Cu^0 [40]:

$$CuO + H_2 \rightarrow Cu^0 + H_2O$$

This direct reaction is considered because it is known that Cu^+ is not a stable intermediate ion to form Cu_2O under these conditions [39]. Also, the absence of TPR signals at higher temperatures for 4Cu0Co/H perhaps indicates that the formation of phases having high interaction with support did not occur.

The TPR profiles of Cu—Co (oxides) mixed catalysts show an important shift of signals to lower temperatures regarding those for single metal catalysts. In these cases the peak of maximum reduction at lower temperatures suggests an interaction between copper and cobalt ions facilitating the chemical reduction. A mixed Cu—Co oxide (isomorphic substitution of Cu^{2+} for Co^{2+} in Co_3O_4) with a spinel type structure ($CuCo_2O_4$) has been proposed according to the literature [41]. It is evident that copper-ions addition in the

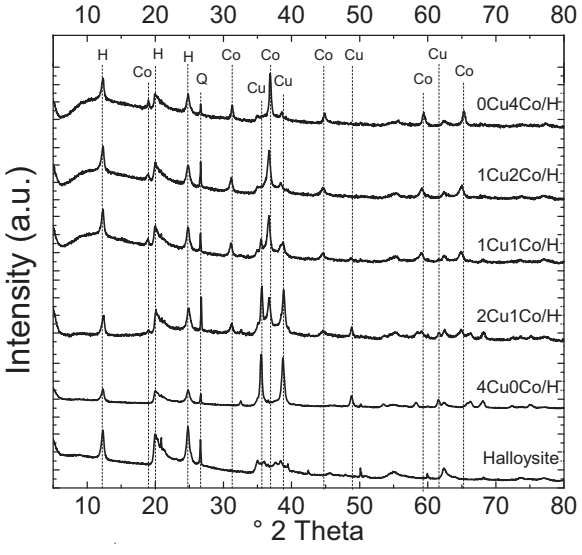

Fig. 1. X-ray diffraction profiles for Cu—Co/halloysite catalysts, varying the Cu/Co molar ratio. H: halloysite, Co: cobalt oxide (Co_3O_4), Cu: copper oxide (CuO) and Q: quartz. In all the catalysts a quantity of 4 mmol of metal/g of halloysite (20 wt%) was used.

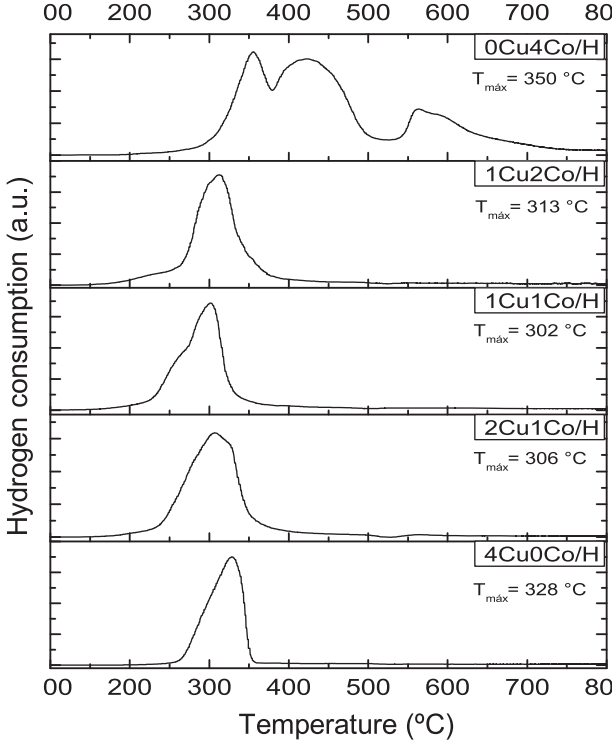

Fig. 2. H_2-TPR profiles for the (20 wt%) Cu—Co/halloysite catalysts, varying the Cu/Co molar ratio.

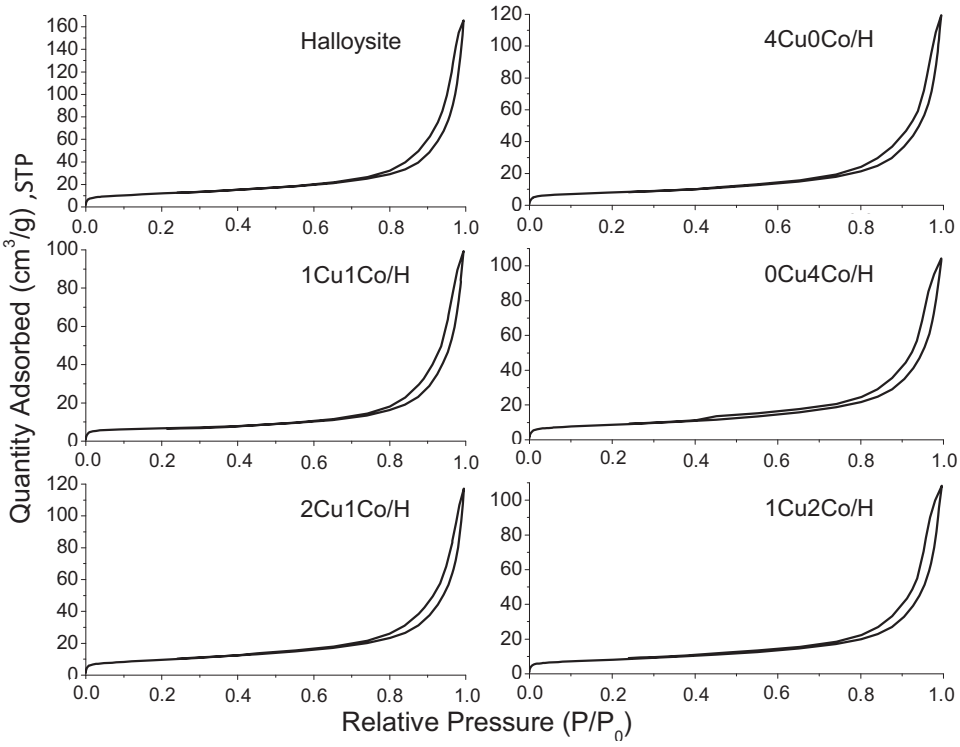

Fig. 3. Adsorption–desorption isotherms for the (20 wt%) Cu—Co/halloysite catalysts, varying the Cu/Co molar ratio.

bimetallic catalyst improves the reducibility of cobalt. This reducing behavior of Cu—Co mixed oxide catalysts is very important for these materials be used in redox reactions.

Bare halloysite (support) did not show a H_2-TPR profile with important intensities to be compared with those obtained for Co, Cu or Cu—Co oxides supported on halloysite. Negligible TPR intensities of the support are associated with its low content of reducible species (lower than 2.081 wt% in the bulk, found by chemical analyses (XRF)), regarding 20 wt% of Cu/Co ions in the surface of the supported catalysts. An amplified TPR profile of this halloysite has been published previously [42], in which no signal is observed below 500 °C.

3.1.4. N_2 adsorption analysis

Fig. 3 shows the adsorption isotherms for both the natural halloysite and synthesized materials. This series of catalysts reveals mixed characteristics of type II/IV isotherms (according to the IUPAC classification), which indicates a predominant existence of meso and macropores. At low pressures, a very small increase in the adsorbed volume occurs, which indicates the presence of micropores in very small amounts. The isotherms show a type H_1 hysteresis, characteristic of materials with cylindrical or tubular pores. None of the cases shows significant modifications in the shape of the adsorption–desorption curve, demonstrating that the textural characteristics of the support predominate.

The values of textural parameters (Table 2) show lower specific surface areas for the catalysts with respect to the clay mineral. In addition, it is observed that the micropore area was not significantly modified, while in all the cases there was a decrease in the mesopore area, indicating that the incorporation of metal oxides probably leads to the formation of aggregates that perhaps block the halloysite mesoporous cavities. It is also observed that the average pore radius is maintained without relevant alteration, i.e., the pore type was conserved. The pore size distribution determined by the BJH method (Fig. 4) shows a peak in the distribution at approximately 110 Å. In all the catalysts, even though a monomodal distribution is maintained with similar shape to the distribution of the support, a decrease in the pore population is observed, indicating that the support porosity really was affected to a greater extent by the incorporation of Co oxides.

3.1.5. Catalytic evaluation

The results of catalytic evaluation for materials prepared with different Cu/Co molar ratios and for the clay mineral without supported species, in the toluene oxidation reaction, are presented in Fig. 5 and Table 2. The temperatures at which 50% or 90% of

Table 2
Textural parameters of the supported catalysts, and parameters of catalytic evaluation (T_{50} and T_{90}) for the total oxidation of toluene using the supported catalysts varying the molar ratio of Cu—Co. Micropore and mesopore areas were determined by *t*-plots, and pore sizes by BJH distributions.

	Micropore area (m^2/g)	Mesopore area (m^2/g)	BET area (m^2/g)	Pore size, BJH (Å)	$T_{50} \pm 2$ °C	$T_{90} \pm 5$ °C
Halloysite	9	33	42	~110	340	–
4Cu0Co/H	9	18	27	75–95	318	358
2Cu1Co/H	5	29	34	75–95	280	314
1Cu1Co/H	11	12	23	75–96	274	308
1Cu2Co/H	6	22	28	75–95	272	301
0Cu4Co/H	10	20	30	75–97	302	318
Pt/γ-Al_2O_3	–	–	–	–	225	237

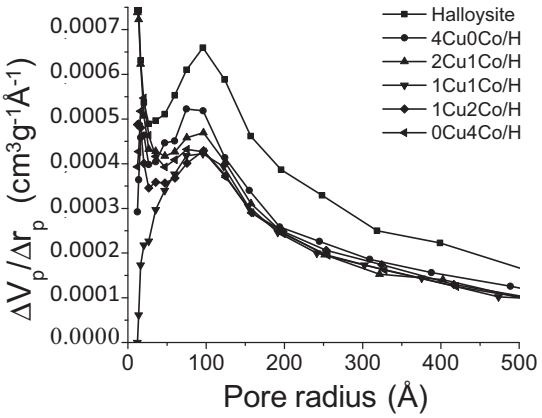

Fig. 4. BJH pore size distributions for the (20 wt%) Cu—Co/halloysite catalysts with different Cu/Co molar ratio.

conversion to CO_2 (T_{50} or T_{90}) are achieved, were used to compare the catalytic activities.

It is evident that all the materials showed a good catalytic activity in the total oxidation of toluene. However, the lowest catalytic performance is obtained with the clay mineral calcined at 400 °C, characterized by a curve strongly inclined toward elevated temperature values, with the highest T_{50} (340 °C) and without reaching 90% conversion. Although the support shows the lowest catalytic conversion, it is an important result because it reveals that the bare halloysite has a significant catalytic activity.

The catalysts prepared with the incorporation of Cu and/or Co oxide species showed a higher activity than that observed for the support. Furthermore, it is clear that the monometallic catalysts present lower catalytic activity than the bimetallic catalysts. The catalyst with only copper (4Cu0Co/H) shows the lowest performance, followed by the material with only cobalt (0Cu4Co/H) (Table 2). It is important to clarify that all the synthesized catalysts present lower activity toward the formation of CO_2 than the catalyst of reference (1% Pt/Al_2O_3).

On the other hand, the lowest values of T_{50} and T_{90} are found for the materials with two metals as the active phase, confirming the strong cooperative effect between those oxides; a 90% conversion of toluene to CO_2 and H_2O is obtained at a temperature of 301 °C for the best of the catalysts. It is important to highlight that all the Cu—Co mixed catalysts exceed 50% of conversion at 280 °C (Table 2). Among these three catalysts, the Cu/Co molar ratios of 1/1 and 1/2 (1Cu1Co/H and 1Cu2Co/H) constitute the most important catalysts. These materials were chosen to study the effect of metal loading between 10 and 40 wt%, always maintaining the same molar ratio.

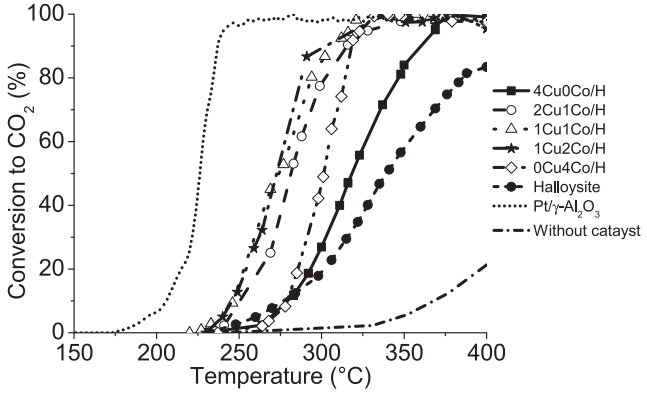

Fig. 5. Catalytic tests for the (20 wt%) Cu—Co/halloysite catalysts with different Cu/Co molar ratio.

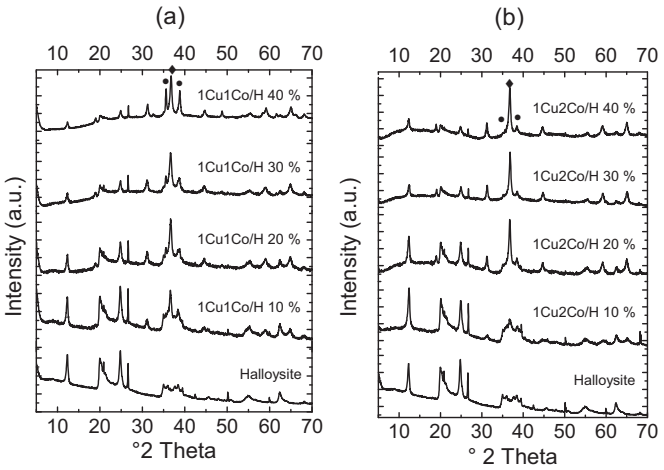

Fig. 6. XRD profiles of the best supported catalysts with different loading of metals (10, 20, 30, 40 wt%). (a) 1Cu1Co/H series and (b) 1Cu2Co/H series. Typical signals of CuO (●) and Co_3O_4 (♦).

The results show that the combination of the copper and cobalt metal ions forming mixed oxides facilitates the total oxidation of toluene to CO_2 and water, and very likely constitutes an important route to obtain excellent catalysts for the removal of VOCs.

3.2. *Effect of metal oxide loading: total nominal content of Cu and Co metals*

3.2.1. *X-ray diffraction*

The typical signals of copper (CuO) and cobalt (Co_3O_4) oxides were observed in the XRD profiles (Fig. 6). For the 1Cu1Co/H bimetallic catalyst series (Fig. 6a), it was observed that the materials with 10, 20 and 30 wt% of active phase showed low intensity for the copper oxide signals, while the material with a 40 wt% loading showed the CuO typical signals increased, revealing the favorable formation of this phase. On the other hand, none of the materials of the 1Cu2Co/H series (Fig. 6b) revealed this behavior, which indicates that this molar ratio facilitates the formation of cobalt oxide or a mixed oxide with the same structure of cobalt oxide that is stable as increasing mass content.

Table 3 shows the particle sizes calculated by the Scherrer equation. It can be observed that the particle sizes of crystallites increase with larger metal loading up to 30 wt%; subsequently, a slight decrease was observed, possibly because of the favorable formation of certain phases as observed by XRD. In order to compare the particle sizes with that of unsupported Cu—Co mixed oxide, this bulk mixed oxide was synthesized and analyzed by X-ray powder diffraction (33 nm in size, obtained by the Scherrer equation). Unsupported Cu—Co mixed oxide was synthesized via thermal decomposition of copper and cobalt nitrates, after drying the mixed aqueous solutions, following the same procedure used to prepare the supported catalysts, but without addition of halloysite. For that synthesis a Cu/Co molar ratio equal to 1/1 (analogous to 1Cu1Co/H catalyst) and calcination temperature of 400 °C were used.

3.2.2. *N_2 physisorption*

The adsorption–desorption isotherms of the catalysts with different metal loadings are shown in Fig. 7. In none of the cases isotherms with significant modifications were observed, verifying the predominance of the same type of pores present in the halloysite. However, as can be seen in Table 3, the values of the textural parameters indicate a decrease in the specific surface area (BET) due to the incorporation of the copper–cobalt oxide species. It is

Table 3
Changes in the particle size (determined by the Scherrer Equation) of metal oxide (active phase) as a consequence of increasing the Cu—Co content. Also, textural parameters of the supported catalysts are shown. Micropore and mesopore areas were determined by *t*-plots, and pore sizes by BJH distributions.

Solid	Ps[a] (±3 nm)	Micropore area (m^2/g)	Mesopore area (m^2/g)	BET area (m^2/g)	Pore radius, BJH (Å)
Halloysite	–	9	33	42	~110
1Cu1Co/H 10%	41	7	30	37	75–95
1Cu1Co/H 20%	47	11	12	23	75–96
1Cu1Co/H 30%	65	6	23	29	75–95
1Cu1Co/H 40%	41	4	17	21	75–97
1Cu2Co/H 10%	33	10	27	37	75–97
1Cu2Co/H 20%	36	6	22	28	75–97
1Cu2Co/H 30%	47	5	22	28	75–97
1Cu2Co/H 40%	33	1	28	29	75–97
Cu—Co[b] mixed oxide (unsupported): 33 nm					

[a] Particle size (nm). Signal corresponding to the (3 1 1) plane of Co_3O_4 (36° 2θ) was used.
[b] Bulk mixed oxide synthesized with a 1/1 Cu/Co molar ratio and calcined at 400 °C.

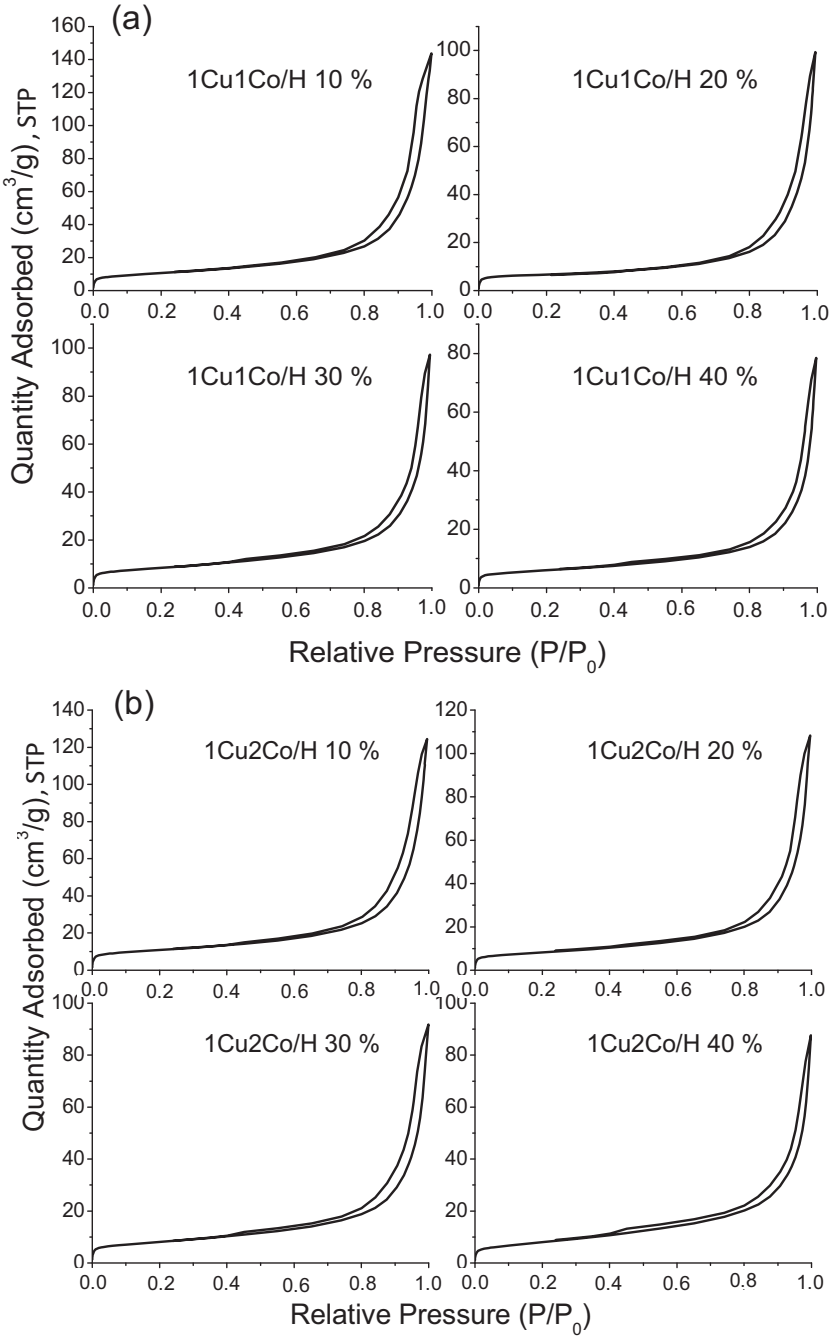

Fig. 7. Adsorption–desorption isotherms for the best catalysts increasing the active phase loading. (a) 1Cu1Co/H series and (b) 1Cu2Co/H series.

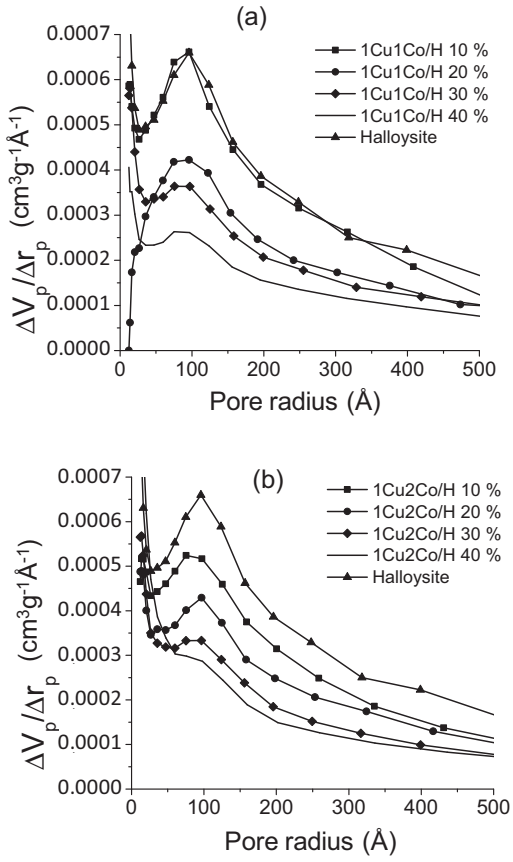

Fig. 8. BJH pore size distributions. Effect of the metal oxide loading. (a) 1Cu1Co/H series and (b) 1Cu2Co/H series.

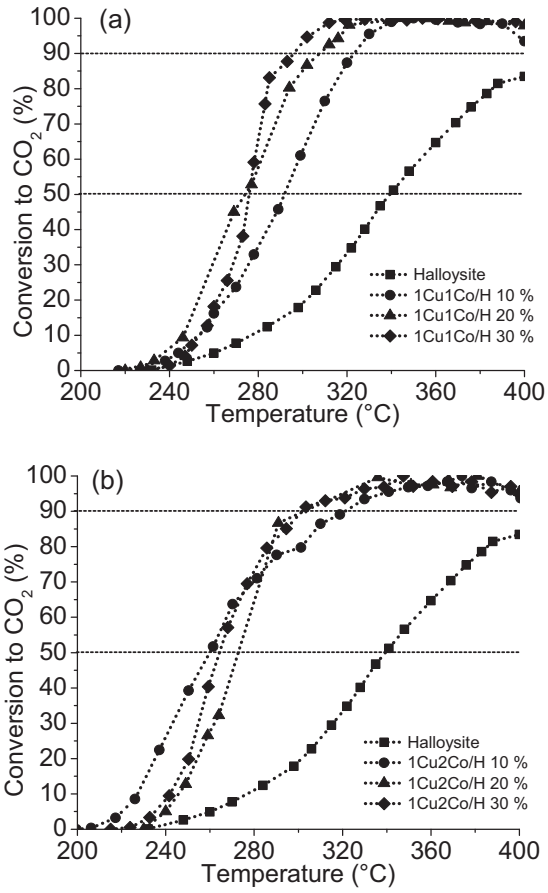

Fig. 9. Effect of the metal oxide loading on the catalytic performance of the Cu—Co/halloysite solids. (a) 1Cu1Co/H series and (b) 1Cu2Co/H series.

also observed that loadings greater than 20% do not cause a larger decrease in the areas.

The pore size distribution calculated by the Barrett–Joyner–Hallenda (BJH) method (Fig. 8) shows a gradual decrease in the mesopores population with increasing the oxide content, although the average pore radius is not modified. These results confirm that higher metal oxide contents favor the formation of a greater amount of aggregates, which leads to a partial blockage of the pores and also to the loss of area.

3.2.3. Catalytic activity

Fig. 9 and Table 4 summarize the effect of the Cu/Co nominal loading on the catalytic performance of the materials in the total oxidation of toluene. For the 1Cu1Co/H catalysts, it is clear that the activity increases with increasing metal oxide content (higher number of active sites); however, for the catalysts containing 20 and 30 wt% of Cu—Co, both the conversion curves and T_{50} values are very close.

As previously described, the copper oxide presents lower catalytic performance than the cobalt oxide, and increasing the metal loading in the 1Cu1Co/H series most likely favors CuO formation, as observed by XRD results; therefore, it is likely that in catalysts with loadings greater than 20 wt%, the preferential formation of that phase leads to moderate catalytic activity. In addition, the possible blockage of mesopores reduces the mass transport toward the active phase; thus, the catalytic performance is affected. As a result, with a loading of 20% for the 1Cu1Co/H series, an optimum balance between the catalytic performance and the amount of the supported species was obtained. On the other hand, in the 1Cu2Co/H series, it is observed that the catalysts with loadings of 10, 20 and 30 wt% of active phase present similar catalytic behavior (characterized by similar values of T_{50} and T_{90}). Thus, based on the results presented and considering the stoichiometric amounts of each metal in these materials, it is possible to conclude that a smaller amount of the CuO phase is most likely contained in this series of catalysts. In addition, it is clear that for this series of catalysts, a metal oxide loading of 10 wt% was enough to obtain the lowest value of T_{50}.

Finally, metal loadings of 20 wt% for the 1Cu1Co/H series and 10 wt% for the 1Cu2Co/H were chosen as the best catalysts for the total oxidation of toluene. Among these materials, the 1Cu2Co/H 10% catalyst showed the best balance between the chemical and textural properties, with a lower active phase content.

3.2.4. Stability evaluation

To verify the structural stability of the support (halloysite) during thermal treatment in the synthesis process and during the catalytic test, X-ray diffraction was used (Fig. 10a). Height ratios between $d_{(001)}$ signal (12.09° 2θ) of the halloysite and that of quartz (26.60° 2θ) in the (20 wt%) 1Cu1Co/H sample diffractograms were evaluated before and after those processes. In addition, transmission electron microscopy was used to observe the presence of nanotubes before and after the synthesis of the catalysts. As can be seen in Fig. 10a and Table 4, no important structural transformations were observed as a result of the process conditions in either the catalyst synthesis (400 °C for 2 h) or the catalytic test (400 °C, air and toluene flow). Moreover, the presence of halloysite nanotubes in the material was confirmed by TEM (Fig. 10b). This result confirms the structural stability of this material during the thermal treatments performed in these two processes.

Table 4
Effect of the nominal metal load on the catalytic parameters of the supported solids, besides ratio between $d_{(001)}$ signal of halloysite (H) and that of quartz (Q) (26.6° 2θ) for the (20 wt%) 1Cu1Co/H solid, before and after the synthesis, and after the catalytic test.

Solid	$T_{50} \pm 2$ °C	$T_{90} \pm 5$ °C	Solid	H/Q	Ps[a] (±3 nm)
1Cu1Co/H 10%	291	322	Halloysite	1.2	–
1Cu1Co/H 20%	274	308	1Cu1Co/H 20% (fresh)	1.3	47
1Cu1Co/H 30%	276	298	1Cu1Co/H 20% (used)	1.2	52
1Cu2Co/H 10%	261	319			
1Cu2Co/H 20%	272	301			
1Cu2Co/H 30%	265	301			

[a] Particle size (nm). Signal corresponding to the (3 1 1) plane of Co_3O_4 (36° 2θ) was used.

Likewise, the stability of the 1Cu1Co/H 20 wt% catalyst was investigated by analyzing the catalytic conversion to CO_2 in a consecutive series of catalytic cycles from 400 to 100 °C. Catalytic conversion of this material was also evaluated continuously at 308 °C (T_{90}) for 9 h. In the first case, four cycles were performed using the same catalyst (Fig. 11a). The conversion data for each cycle showed no appreciable changes in both T_{50} and T_{90} values. These observations indicate that this catalyst exhibited elevated catalytic stability in the reuse tests.

Fig. 11b shows the evolution of the catalytic conversion over time at 308 °C (T_{90}) using the 1Cu1Co/H 20% catalyst. This temperature was chosen because it generated a conversion less than 100%, offering higher sensitivity to a possible change in the catalyst performance. These experiments showed that the conversion of toluene to CO_2 remained stable (90 ± 2%), without appreciable deactivation. By combining these results with those obtained by XRD, it is possible to establish a good stability for the catalysts.

3.3. Studying the active phase of catalysts

Bulk (unsupported) single oxides (CuO, Co_3O_4) and the bulk Cu–Co mixed oxide ($CuCo_2O_3$) were synthesized by thermal decomposition of the corresponding nitrates (after drying the mixed aqueous solutions, the solids were calcined at 400 °C), following a similar procedure to that used for preparing the supported catalysts, but without addition of halloysite. For synthesizing the bulk Cu–Co mixed oxide a Cu/Co molar ratio equal to 1/1 was employed (analogous to the 1Cu1Co/H catalyst). A mechanical mixture containing copper oxide (CuO), cobalt oxide (Co_3O_4) and halloysite was also prepared maintaining a Cu/Co molar ratio of 1/1 in order to compare the results. This material was named MO and its total loading of metal is 20 wt%. The characterization of these solids was performed according to previously described procedures (Section 2.2).

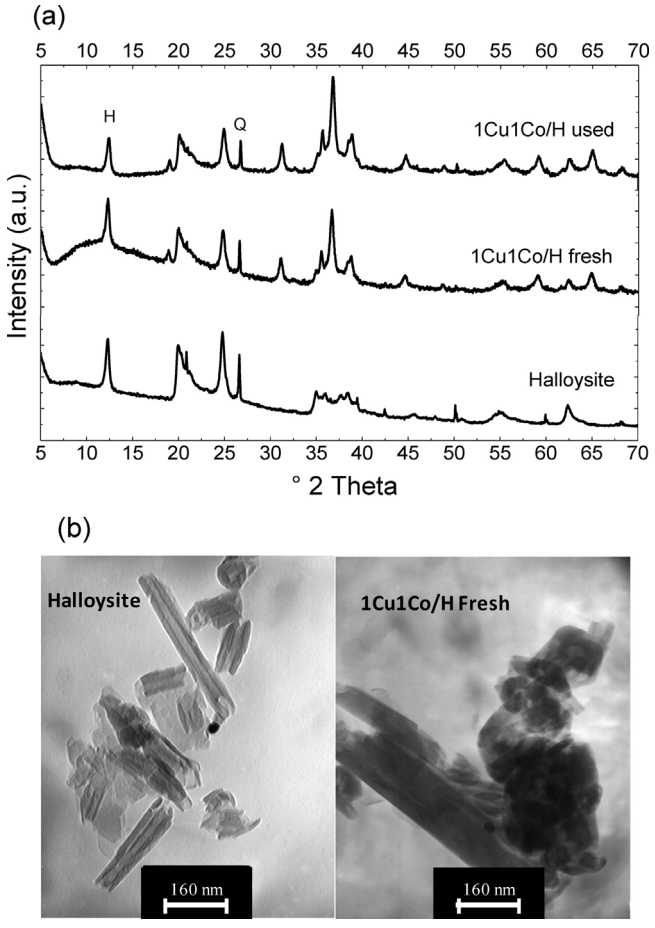

Fig. 10. Structural stability assessment of the support and the (20 wt%) 1Cu1Co/H catalyst. (a) XRD evidences after the synthesis and a catalytic test, (b) nanotubes observed by TEM before and after the catalyst synthesis.

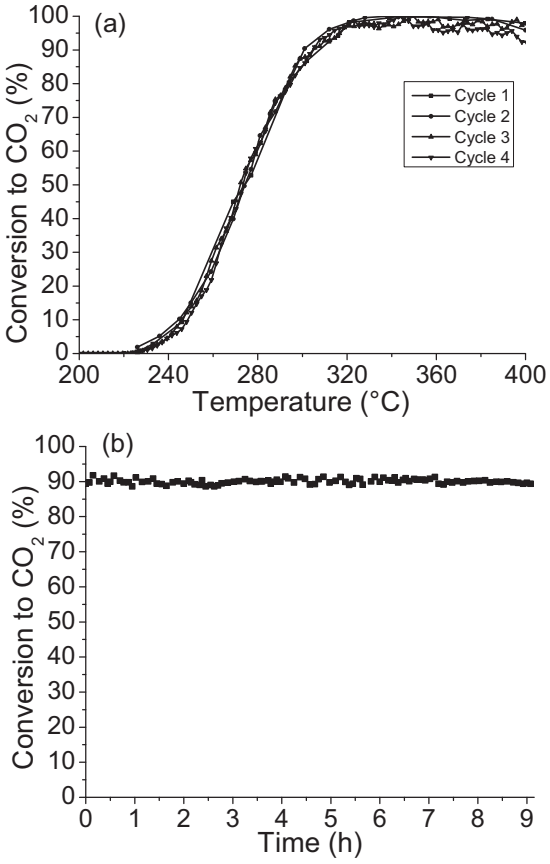

Fig. 11. Stability tests for the catalyst (20 wt%) 1Cu1Co/H on the total oxidation of toluene. (a) Reuse cycles and (b) conversion of toluene over time.

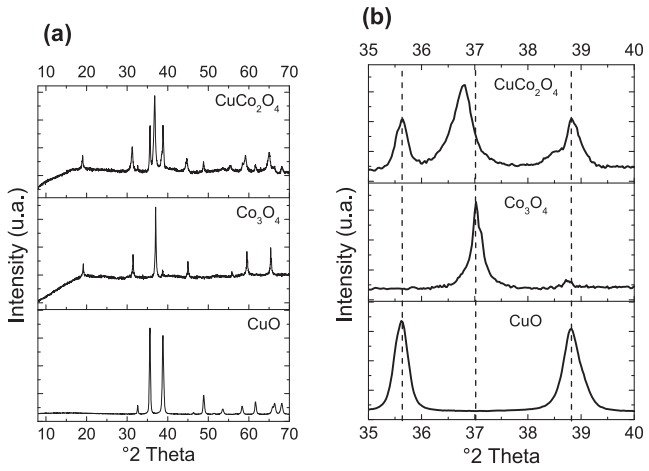

Fig. 12. X-ray diffraction profiles of bulk (unsupported) oxides. (a) Complete profiles and (b) amplified 35–40° 2θ ranges.

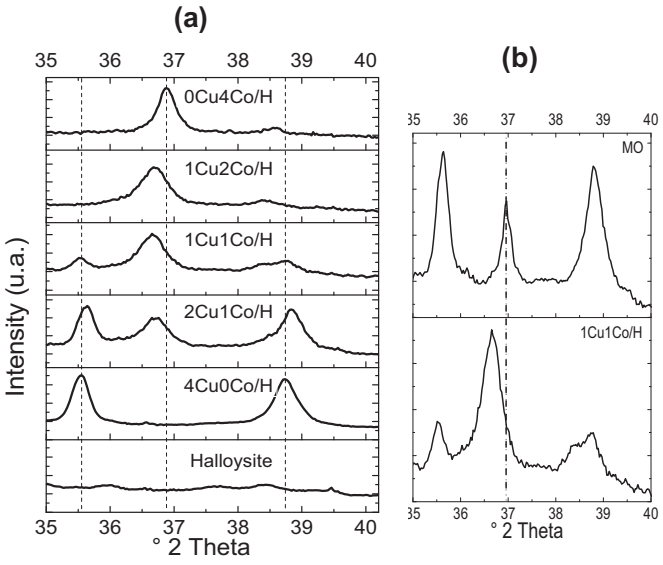

Fig. 13. Detailed X-ray diffraction profiles of supported catalysts showing the signals of metal oxides and the shift of peak positions as consequence of the isomorphic substitution. (a) (20 wt%) Cu—Co/H solids and (b) MO solid compared with (20 wt%) 1Cu1Co/H.

X-ray diffraction profiles for bulk oxides (Fig. 12) show the typical signals of CuO (monoclinic), Co_3O_4 (cubic), and $CuCo_2O_3$ (cubic), verifying the successful synthesis of such materials. Assignment of signals was carried out by comparison with previous works in the literature [35,41]. According to the literature, Co_3O_4, and $CuCo_2O_3$ crystallized as a spinel-type structure. This cubic cell structure has a characteristic XRD peak at 37.0° 2θ in the case of Co_3O_4, which correspond to the plane (3 1 1). For the synthesized cobalt oxide, this signal was clearly identified at that position, but a significant shift toward 36.7° 2θ was observed in the XRD pattern of mixed Cu—Co oxide (Fig. 12b). The shift of that peak to lower (2θ) angle corresponds to an increase of the lattice parameter (unit cell dimension), verifying the isomorphic substitution of Cu^{2+} (ionic radius = 0.87 Å [43]) for Co^{2+} (ionic radius = 0.72 Å [43]) in the tetrahedral positions of the cobalt oxide original structure to form $CuCo_2O_3$. An expansion of the cell parameter was observed going through Co_3O_4 (a = 8.047 Å) to $CuCo_2O_3$ (a = 8.094 Å). According to the literature [41], it is possible to differentiate these two oxides on the basis of small changes (about 0.02 Å) in the size of the unit cell. On the other hand, two peaks (35.6° 2θ and 38.8° 2θ) characteristic of (0 0 2) and (1 1 1) planes of CuO, having less intensity that the peak at 37.0° 2θ, were observed accompanying the central peak of $CuCo_2O_3$ in the XRD profile of Cu—Co mixed oxide. This result indicates that a mixture of both $CuCo_2O_3$ and CuO was obtained in the synthesized material. Higher intensity of the $CuCo_2O_3$ central peak (37.0° 2θ) regarding CuO signals perhaps is related to a higher quantity of the Cu—Co mixed oxide spinel structure.

A similar change in the cell parameter of the supported Cu—Co mixed oxide, compared to that of supported cobalt oxide, was observed as detailed in Fig. 13a. However, although the mechanical mixture of single oxides with halloysite (material MO) showed the typical signals of components (Co_3O_4, CuO and halloysite), no shift for the 37.0° 2θ position was observed in the XRD pattern (Fig. 13b). Additionally, CuO peaks were again observed in the XRD patterns of supported Cu—Co mixed oxides. Furthermore, XRD profile of MO sample shows a higher intensity for CuO peaks, contrary to the intensity ratios observed for the 1Cu1Co/H catalyst (Fig. 13b). This result clearly shows an important difference between a mechanical mixture of the oxides and the Cu—Co mixed oxide synthesized by the chemical method.

It is important to take into account that in the present work the catalysts with better catalytic performance on the toluene oxidation have been those whose metal-oxide active phase contained the $CuCo_2O_3$ structure. In order to check the reducing behavior of bulk oxides synthesized, the H_2-TPR analyses were carried out (Fig. 14).

Typical different TPR profiles were observed for Co_3O_4, $CuCo_2O_3$, and CuO oxides, indicating different characteristics on the nature and structure. Reducing processes involved in the reaction were previously discussed (Section 3.1.3). H_2-TPR profiles show lower reduction temperatures for the $CuCo_2O_3$ and 1Cu1Co/H materials, verifying the beneficial effect on redox-properties of the bimetallic system when Cu—Co mixed oxide was synthesized. Mechanical mixture (MO) clearly shows a bimodal TPR curve revealing the independent presence of both cobalt oxide and copper oxide. These results, and those above discussed on the XRD suggest a direct relationship between the formation of $CuCo_2O_3$ structure and the cooperative effect observed for the catalytic results.

The catalytic performance of bulk synthesized oxides in the total oxidation of toluene was carried out to verify the effect of bimetallic system regarding single oxides (Fig. 15). Once more the catalytic conversion of Cu—Co mixed oxide ($CuCo_2O_4$) was better than those of single oxides. Lower temperatures of conversion (high catalytic activity) were observed for Co_3O_4 than for CuO, showing a better catalytic activity of cobalt oxide. However, the supported catalyst (1Cu1Co/H) showed higher catalytic conversion than the

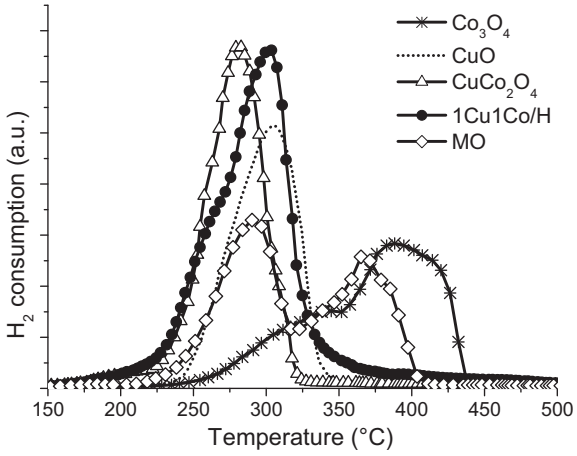

Fig. 14. H_2-TPR profiles of the bulk (unsupported) oxides, and for the mixture of oxides (MO) compared to the (20 wt%) 1Cu1Co/H catalyst.

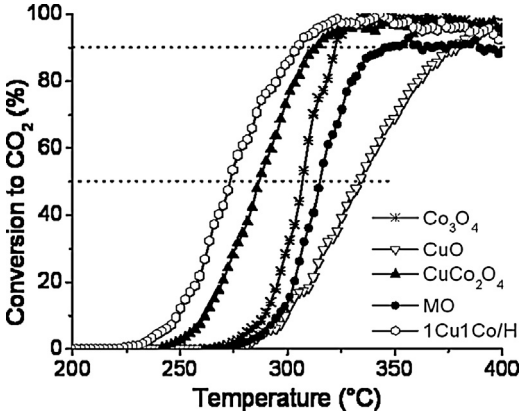

Fig. 15. Catalytic conversions (total oxidation of toluene) for the bulk oxides, and their comparison with the conversions of MO and (20 wt%) 1Cu1Co/H catalyst.

unsupported synthesized solid, revealing the beneficial effect of the support. The material MO showed lower catalytic conversion than bulk cobalt oxide, which is a consequence of the lesser quantity of metal oxides (20%) contained in the mixture. According to the synthesis and quantity of metals in the bulk oxides, these catalytic results clearly show a correlation between $CuCo_2O_4$ structure and the high catalytic performance of the materials, confirming that a cooperative effect is result of the formation of this spinel-type structure.

4. Conclusions

The X-ray diffraction results revealed that the species formed from cobalt and/or copper in the catalysts supported on halloysite are CuO and Co_3O_4. The catalytic support (halloysite) determined the textural properties of the synthesized materials, but minor losses of the surface area were observed as consequence of partial obstructions of pores because of metal oxide species. The supported catalysts, using Cu and/or Co oxides as the active phase, showed elevated activity for the complete combustion of toluene at moderate temperatures. Among the monometallic catalysts, the cobalt catalyst showed better performance than that of copper. A cooperative effect was observed between the copper and cobalt oxides, and Cu/Co molar ratios of 1/1 and 1/2 showed the highest catalytic activity in the studied reaction. For copper and cobalt mixed oxides, it was found that formation of a separate CuO phase decreased the catalytic performance; therefore the 1/2 Cu/Co ratio gave better results. Both 1Cu1Co/H 20 wt% and 1Cu2Co/H 10 wt% catalysts had the best balance of chemical, textural and catalytic properties. Finally, the halloysite mineral showed a structural stability suitable to be considered as a good support, with excellent properties for both the synthesis of catalysts and the catalytic oxidation of toluene.

Acknowledgements

This work was performed with the logistic and financial support of the Faculty of Science of the National University of Colombia. A part of this work was developed at the 125-Lab (Lab-DRES: Laboratorio de Diseño y Reactividad de Estructuras Sólidas) of the UNAL-Bogotá.

References

[1] G.S. Pozan, J. Hazard. Mater. 221–222 (2012) 124–130.
[2] L.F. Liotta, Appl. Catal. B 100 (2010) 403–412.
[3] S. Todorova, G. Kadinov, K. Tenchev, A. Caballero, J.P. Holgado, R. Pereñíguez, Catal. Lett. 129 (2009) 149–155.
[4] F. Kovanda, K. Jirátová, Appl. Clay Sci. 53 (2011) 305–316.
[5] J.J. Spivey, Ind. Eng. Chem. Res. 26 (1987) 2165–2180.
[6] S.M. Saqer, D.I. Kondarides, X.E. Verykios, Appl. Catal. B 103 (2011) 275–286.
[7] S. Todorova, A. Naydenov, H. Kolev, J.P. Holgado, G. Ivanov, G. Kadinov, A. Caballero, Appl. Catal. A 413–414 (2012) 43–51.
[8] P. Li, C. He, J. Cheng, C.Y. Ma, B.J. Dou, Z.P. Hao, Appl. Catal. B 101 (2011) 570–579.
[9] C.H. Wang, Chemosphere 55 (2004) 11–17.
[10] M.H. Castaño, R. Molina, S. Moreno, J. Mol. Catal. A 370 (2013) 167–174.
[11] C. Ma, Z. Mu, C. He, P. Li, J. Li, Z. Hao, J. Environ. Sci. 23 (2011) 2078–2086.
[12] F. Wyrwalski, J.F. Lamonier, S. Siffert, L. Gengembre, A. Aboukaïs, Catal. Today 119 (2007) 332–337.
[13] A. Kołodziej, J. Łojewska, J. Tyczkowski, P. Jodłowski, W. Redzynia, M. Iwaniszyn, S. Zapotoczny, P. Kuśtrowski, Chem. Eng. J. 200–202 (2012) 329–337.
[14] B. Solsona, T.E. Davies, T. Garcia, I. Vázquez, A. Dejoz, S.H. Taylor, Appl. Catal. B 84 (2008) 176–184.
[15] F. Wyrwalski, J.F. Lamonier, S. Siffert, A. Aboukaïs, Appl. Catal. B 70 (2007) 393–399.
[16] I. Yuranov, N. Dunand, L. Kiwi-Minsker, A. Renken, Appl. Catal. B (2002) 183–191.
[17] V.G. Milt, E.A. Lombardo, M.A. Ulla, Appl. Catal. B 37 (2002) 63–73.
[18] H. Wu, L. Wang, Z. Shen, J. Zhao, J. Mol. Catal. A 351 (2011) 188–195.
[19] Q. Liu, L.C. Wang, M. Chen, Y. Cao, H.Y. He, K.N. Fan, J. Catal. 263 (2009) 104–113.
[20] F. Kovanda, T. Rojka, J. Dobešová, V. Machovič, P. Bezdička, L. Obalová, K. Jirátová, T. Grygar, J. Solid State Chem. 179 (2006) 812–823.
[21] S.S.T. Bastos, J.J.M. Órfão, M.M.A. Freitas, M.F.R. Pereira, J.L. Figueiredo, Appl. Catal. B 93 (2009) 30–37.
[22] J.G. Carriazo, L.F. Bossa-Benavides, E. Castillo, Quim. Nova 35 (2012) 1101–1106.
[23] A. Pérez, M. Montes, R. Molina, S. Moreno, Appl. Catal. A 408 (2011) 96–104.
[24] S. Somekawa, T. Hagiwara, K. Fujii, M. Kojima, T. Shinoda, K. Takanabe, K. Domen, Appl. Catal. 409–410 (2011) 209–214.
[25] P. Serp, E. Castillejos, ChemCatChem 2 (2010) 41–47.
[26] P. Luo, Y. Zhao, B. Zhang, J. Liu, Y. Yang, J. Liu, Water Res. 44 (2010) 1489–1497.
[27] S. Barrientos-Ramírez, E.V. Ramos-Fernández, J. Silvestre-Albero, A. Sepúlveda-Escribano, M.M. Pastor-Blas, A. González-Montiel, Microporous Mesoporous Mater. 120 (2009) 132–140.
[28] M.T. Viseras, C. Aguzzi, P. Cerezo, C. Viseras, C. Valenzuela, Microporous Mesoporous Mater. 108 (2008) 112–116.
[29] A. Vaccari, Catal. Today 41 (1998) 53–71.
[30] A. Vaccari, Appl. Clay Sci. 14 (1999) 161–198.
[31] L. Wang, J. Chen, L. Ge, Z. Zhu, V. Rudolph, Energy Fuels 25 (2011) 3408–3416.
[32] Z.Y. Cai, M.Q. Zhu, H. Dai, Y. Liu, J.X. Mao, X.Z. Chen, C.H. He, Adv. Chem. Eng. Sci. 1 (2011) 15–19.
[33] D. Papoulis, S. Komarneni, D. Panagiotaras, E. Stathatos, D. Toli, K.C. Christoforidis, M. Fernandez-Garcia, H. Li, S. Yin, T. Sato, H. Katsuki, Appl. Catal. B 132–133 (2013) 416–422.
[34] Y. Zhang, J. Ouyang, H. Yang, Appl. Clay Sci. 95 (2014) 252–259.
[35] T. Palacios-Hernández, G.A. Hirata-Flores, O.E. Contreras-López, M.E. Mendoza-Sánchez, I. Valeriano-Arreola, E. González-Vergara, M.A. Méndez-Rojas, Inorg. Chim. Acta 392 (2012) 277–282.
[36] L. He, H. Berntsen, E. Ochoa-Fernández, J. Walmsley, E. Blekkan, D. Chen, Top. Catal. 52 (2009) 206–217.
[37] M. Gabrovska, R. Edreva-Kardjieva, K. Tenchev, P. Tzvetkov, A. Spojakina, L. Petrov, Appl. Catal. A 399 (2011) 242–251.
[38] H.G. El-Shobaky, Appl. Catal. A 278 (2004) 1–9.
[39] A.A. Khassin, T.M. Yurieva, G.N. Kustova, I.S. Itenberg, M.P. Demeshkina, T.A. Krieger, L.M. Plyasova, G.K. Chermashentseva, V.N. Parmon, J. Mol. Catal. A 168 (2001) 193–207.
[40] A.F. Lucrédio, G. Jerkiewicz, E.M. Assaf, Appl. Catal. B 84 (2008) 106–111.
[41] W.M. Shaheen, A.A. Ali, Mater. Res. Bull. 36 (2001) 1703–1716.
[42] A.M. Carrillo, J.G. Carriazo, S. Moreno, R.A. Molina, Rev. Mex. Ing. Quím. 13 (2014) 563–571.
[43] R.D. Shannon, Acta Crystallogr. A 32 (1976) 751–767.